

Theory of diffracted channeling radiation

R. Yabuki and H. Nitta*

Department of Physics, Tokyo Gakugei University, Koganei, Tokyo 184-8501, Japan

T. Ikeda and Y. H. Ohtsuki

Department of Physics, Waseda University, Shinjuku, Tokyo 169-8555, Japan

(Received 1 November 2000; published 16 April 2001)

Monochromatic x-ray emission is predicted for MeV channeled electrons/positrons. The mechanism of this radiation is intuitively understood as diffraction of virtual channeling radiation into the direction of the Bragg angles with respect to the electron beam. Our numerical calculations predict that spectral density of the emitted x rays is about ten times larger than that of parametric x-ray radiation.

DOI: 10.1103/PhysRevB.63.174112

PACS number(s): 61.85.+p, 41.60.-m

I. INTRODUCTION

There is no doubt that making a monochromatic, intense, tunable, as well as compact x-ray source will bring further development to various fields of science, technology, and medicine. At present, channeling radiation (CR) is one of the candidates for such an x-ray source. Indeed, CR up to ~ 0.1 photon per e^- per sr. has been observed,¹ demonstrating that CR can be used as a practical x-ray source.

Unfortunately, CR has a large continuous background radiation due to incoherent bremsstrahlung. Therefore, we need a monochromator for extraction. Furthermore, since CR is emitted along the electron beam, we need equipment for sweeping out the electrons. This equipment will cause the x-ray generating system based on CR to become rather complex and large.

Recently, a new type of coherent x-ray radiation from crystals, called ‘‘parametric x-ray radiation’’ (PXR), has become a new candidate for the compact x-ray source of the future. In PXR, it is not difficult to extract x rays because they are emitted in the direction satisfying the Bragg conditions. Moreover, the background radiation in PXR is negligibly small.² However, the intensity of PXR is about 10^{-3} – 10^{-4} times smaller than that of CR.

Taking into account the advantages in CR and PXR, it is interesting to consider the possible use of the target crystal itself as a monochromator for CR. As is well known, a MeV channeled electron emits CR spontaneously by changing its transverse energy from $E_{\perp,i}$ to $E_{\perp,f}$. Due to the Doppler shift, the frequency of CR emitted in the forward direction becomes $\omega_{CR} \approx 2\gamma^2\Omega_{if}$, where γ is the Lorentz factor and $\Omega_{if} = (E_{\perp,i} - E_{\perp,f})/\hbar$. Let ω_B represent the frequency of photons satisfying the Bragg condition $\omega_B = c|\mathbf{g}|/(2 \sin \theta_B)$, where \mathbf{g} is the reciprocal-lattice vector and θ_B the Bragg angle. If the condition

$$\omega_{CR} \approx \omega_B \quad (1.1)$$

is satisfied, the CR photon will be diffracted in the crystal. In other words, we have an x-ray emission as a result of diffraction of virtual CR. We call this radiation process ‘‘diffracted channeling radiation’’ (DCR).

CR taking into account diffraction is discussed in Ref. 3 and calculated using a kinematical theory.^{4,5} However, neither the absolute value nor the angular distribution has been given. This is because the kinematical theory results in a divergence at the resonance condition of Eq. (1.1).^{4,5}

In this paper, we use the dynamical theory for x-ray photons, predicting various properties of DCR. It is shown that, in comparison with PXR, the spectral density of DCR is very large and the width of the angular distribution is very narrow. The peak intensity of DCR is about 10 times larger than that of PXR.

II. THEORY

A. Frequency of diffracted channeling radiation

In this section, we derive the expression for the frequency of DCR from the energy and momentum-conservation equations. When a photon is emitted from a channeled electron, the photon energy $\hbar\omega$ is given as the difference of the initial and final energy of the electron as

$$E_i - E_f = \hbar\omega, \quad (2.1)$$

where $E_i \approx E(\mathbf{p}_{\parallel}) + E_{\perp,i}$, $E_f \approx E(\mathbf{p}'_{\parallel}) + E_{\perp,f}$, $E(\mathbf{p}_{\parallel}) = \sqrt{(c\mathbf{p}_{\parallel})^2 + m^2c^4}$, and \mathbf{p}_{\parallel} is the momentum along the channel. The momentum is conserved only in the direction parallel to the channel

$$\mathbf{p}_{\parallel} - \mathbf{p}'_{\parallel} = \hbar(\mathbf{k}_{\parallel} + \mathbf{g}_{\parallel}), \quad (2.2)$$

because the transverse state of the channeled electron is bound. From Eqs. (2.1) and (2.2), under the condition satisfying $\hbar\omega \ll E_i, E_f$, we obtain

$$\omega = \frac{\mathbf{g} \cdot \mathbf{v}_{\parallel} + \Omega_{if}}{1 - \beta_{\parallel}^* \cos \Theta}, \quad (2.3)$$

where $\omega = c^*|\mathbf{k}|$, \mathbf{k} is the wave vector of the photon, $c^* = c/\sqrt{\varepsilon_0}$, ε_0 is the average dielectric constant, $\beta_{\parallel}^* = v_{\parallel}/c^*$, \mathbf{v}_{\parallel} the velocity of the electron along the channel, and Θ the observation angle.

If $\Omega_{if} = 0$, Eq. (2.3) reduces to the well-known formula for the frequency of PXR⁶

$$\omega = \frac{\mathbf{g} \cdot \mathbf{v}_{\parallel}}{1 - \beta_{\parallel} \cos \Theta}. \quad (2.4)$$

On the other hand, if $\mathbf{g} = 0$, then Eq. (2.3) reduces to the expression of the CR frequency:^{8,16}

$$\omega = \frac{\Omega_{if}}{1 - \beta_{\parallel}^* \cos \Theta}. \quad (2.5)$$

It should be noted that the approximated expression $\omega \approx 2\gamma^2\Omega_{if}$ at the forward direction is modified to

$$\omega \approx \frac{2\Omega_{if}}{\gamma^{-2} + |\chi_0(\omega)|}, \quad (2.6)$$

if $\sqrt{|\chi_0(\omega)|} \sim 1/\gamma$ is satisfied.¹⁶ Equation (2.3) may be considered as a unified expression for the frequencies of CR, PXR, and DCR.

It is worthwhile to mention that Eq. (2.3) is not only held for the bound-bound transitions but also for the free-free and free-bound transitions. For example, let us consider the free-free transitions. As shown by Andersen⁷ and in Ref. 8, in this case we may expect coherent bremsstrahlung for $\mathbf{g} = 0$. Correspondingly, for $\mathbf{g} \neq 0$, we may have ‘‘diffracted coherent bremsstrahlung.’’⁹ We will not discuss further this possibility but concentrate on DCR from now on.

B. Radiation processes and their matrix elements

In this section we derive the radiation probability for DCR. We start with the Fermi golden rule,

$$w_{IF} = \frac{2\pi}{\hbar} |\langle F | H_{int} | I \rangle|^2 \rho_F, \quad (2.7)$$

where I and F represent the initial and final states of the system as a whole, respectively, and ρ_F the density of the final state.

For simplicity, from now on we consider planar channeling of electrons. In our case, the effect of spin is negligibly small.⁶ Then the Hamiltonian for the interaction between the channeled electron and the photon field may be given by

$$H_{int} = -\frac{e}{\gamma mc} \mathbf{A} \cdot \hat{\mathbf{p}}, \quad (2.8)$$

where $\hat{\mathbf{p}}$ is the momentum operator. The photon field \mathbf{A} is given in a form of the Bloch wave (see the appendix)

$$\mathbf{A}(\mathbf{r}) = \sum_{\mathbf{k}} \sum_{\mathbf{g}} \mathbf{A}_{\mathbf{g}} \exp[i(\mathbf{k} + \mathbf{g}) \cdot \mathbf{r}] + \text{c.c.} \quad (2.9)$$

The wave function for the planar-channeled electron is given as¹⁶

$$\psi^{(s)}(\mathbf{r}) = \frac{1}{\sqrt{L_x L_z}} \varphi_n(y) e^{i\mathbf{p}_{\parallel} \cdot \mathbf{r}_{\parallel} / \hbar}, \quad (2.10)$$

where $s = (n, \mathbf{p})$ and L_x and L_z are the normalization constants. The factor $\exp(i\mathbf{p}_{\parallel} \cdot \mathbf{r}_{\parallel} / \hbar) / \sqrt{L_x L_z}$ describes the free

state along the channel and $\varphi_n(y)$ the transverse state obtained as a solution of the transverse Schrödinger equation

$$\left[\frac{\hat{\mathbf{p}}_{\perp}^2}{2\gamma m} + V(y) \right] \varphi_n(y) = E_{\perp, n} \varphi_n(y). \quad (2.11)$$

Since the Lindhard continuum potential $V(y)$ is periodic, $\varphi_n(y)$ is written in the form of the Bloch wave

$$\varphi_n(y) = \frac{1}{\sqrt{L_y}} \sum_G C_G^{(n)}(p_y) \exp[i(p_y / \hbar + G)y], \quad (2.12)$$

where G is the reciprocal-lattice vector associated with the channel planes.

Using Eqs. (2.9) and (2.10), the matrix element may be decomposed into two parts:

$$\begin{aligned} & \langle F | H_{int} | I \rangle \\ &= -\langle \varphi_f, \mathbf{p}_{\parallel} | \frac{e}{\gamma mc} [\mathbf{A}_0^* \exp(-i\mathbf{k} \cdot \mathbf{r})] \cdot \hat{\mathbf{p}} | \varphi_i, \mathbf{p}_{\parallel} \rangle \\ & \quad - \langle \varphi_f, \mathbf{p}_{\parallel} | \frac{e}{\gamma mc} \sum_{\mathbf{g}(\neq 0)} \{\mathbf{A}_{\mathbf{g}}^* \exp[-i(\mathbf{k} + \mathbf{g}) \cdot \mathbf{r}]\} \cdot \hat{\mathbf{p}} | \varphi_i, \mathbf{p}_{\parallel} \rangle \\ & \equiv M_0^{(if)} + \sum_{\mathbf{g}(\neq 0)} M_{\mathbf{g}}^{(if)}. \end{aligned} \quad (2.13)$$

The term $M_0^{(ii)}$ corresponds to the emission of a photon without changing the transverse state (i.e., the *intranband transition*). Only the momentum along the channel changes in this case because the transverse state is bound. As we have $\mathbf{g} = 0$ and $\Omega_{ii} = 0$ for this transition, Eq. (2.3) reduces to the Čerenkov condition $1 - \beta_{\parallel}^* \cos \Theta = 0$. Therefore, $M_0^{(ii)}$ represents the Čerenkov radiation under the channeling condition. Of course, as x rays do not satisfy the Čerenkov condition, $M_0^{(ii)}$ does not contribute in our problem.

For the condition $i \neq f$, $M_0^{(if)}$ represents the normal CR. In a strict sense, a certain effect of diffraction may take place because in the two-wave approximation (see the appendix), \mathbf{A}_0 has a form of the superposition of two plane waves on the slightly different energy branches. However, since the difference of the energies is of the order of $|\chi_{\mathbf{g}}| \sim 10^{-4} - 10^{-6}$ this dynamical effect on CR may be usually neglected.

The second term in Eq. (2.13), $M_{\mathbf{g}}^{(if)}$, represents the emission of a diffracted photon. The matrix element $M_{\mathbf{g}}^{(ii)}$, where the transition of the channeled electron is *intranband*, gives PXR under channeling conditions (PXRC). PXRC is different from the normal PXR in that its matrix element includes the form factor of channeling states. Numerically however, as we will discuss in Sec. III, the difference between PXRC and PXR is rather small.

The matrix element $M_{\mathbf{g}}^{(if)}$ ($i \neq f$), which is of our present interest, represents the emission of a diffracted photon due to the *interband transition* between the transverse states (DCR). In the next section, we derive the radiation probability of DCR and PXRC by calculating $M_{\mathbf{g}}^{(if)}$ in more detail.

C. Analytical expression of PXR and DCR

From Eqs. (2.8), (2.10), and (2.13), we obtain the matrix element for the emission of a diffracted photon

$$M_{-\mathbf{g}}^{(if)} = -\left(\frac{e}{c}\right) \left[(\mathbf{A}_{-\mathbf{g}}^* \cdot \mathbf{v}_{\parallel}) \langle \varphi_f | e^{-i(\mathbf{k}-\mathbf{g})_y y} | \varphi_i \rangle + \frac{1}{\gamma m} (\mathbf{A}_{-\mathbf{g}}^*)_y \langle \varphi_f | e^{-i(\mathbf{k}-\mathbf{g})_y y} \hat{p}_y | \varphi_i \rangle \right] \times \delta(\mathbf{p}_{\parallel} - \mathbf{p}'_{\parallel} | \hbar \mathbf{k}_{-\mathbf{g}\parallel}), \quad (2.14)$$

where $\hat{p}_y = -i\hbar(d/dy)$, $(\mathbf{A}_{-\mathbf{g}}^*)_y$ and $(\mathbf{k}-\mathbf{g})_y$ are the y components of $\mathbf{A}_{-\mathbf{g}}^*$ and $\mathbf{k}-\mathbf{g}$, respectively, and $\delta(A|B)$ the Kronecker delta. Using the relation $(-i\hbar/\gamma m)\hat{p}_y = [\hat{H}_y, y]$, Eq. (2.14) is rewritten as

$$M_{-\mathbf{g}}^{(if)} = -\left(\frac{e}{c}\right) \left[(\mathbf{A}_{-\mathbf{g}}^* \cdot \mathbf{v}_{\parallel}) \langle \varphi_f | e^{-i(\mathbf{k}-\mathbf{g})_y y} | \varphi_i \rangle + i(\mathbf{A}_{-\mathbf{g}}^*)_y \Omega_{if} \langle \varphi_f | y | \varphi_i \rangle \right] \delta(\mathbf{p}_{\parallel} - \mathbf{p}'_{\parallel} | \hbar \mathbf{k}_{-\mathbf{g}\parallel}). \quad (2.15)$$

As mentioned in Sec. II B, Eq. (2.15) includes two types of transitions: the intraband transition ($i=f$) and the interband transition ($i \neq f$).

First, we consider the intraband transition. From Eq. (2.15), we obtain

$$M_{-\mathbf{g}}^{(ii)} = -\left(\frac{e}{c}\right) (\mathbf{A}_{-\mathbf{g}}^* \cdot \mathbf{v}_{\parallel}) F_{ii} [(\mathbf{k}-\mathbf{g})_y] \delta(\mathbf{p}_{\parallel} - \mathbf{p}'_{\parallel} | \hbar \mathbf{k}_{-\mathbf{g}\parallel}), \quad (2.16)$$

where

$$F_{ii}(q) = \langle \varphi_i | e^{-iqy} | \varphi_i \rangle \quad (2.17)$$

is the form factor for the channeling state that represents the effect of channeling on PXR. If we substitute φ_i by the plane wave $\exp(ip_y y/\hbar)/\sqrt{L_y}$, the form factor becomes the Kronecker delta $\delta(p_y - p'_y | \hbar q)$.¹⁰ In this case, Eq. (2.16) reduces to the ordinary PXR matrix element⁶ and within the two-wave approximation, we obtain the dynamical expression of the radiation probability of PXR per unit length after summing up the final momentum of the channeled electron^{11,12}

$$\left(\frac{dN}{d\theta_x d\theta_y dz} \right)_{PXR} = \frac{\alpha \omega_B}{4\pi c \sin^2 \theta_B} \times \left(\frac{\theta_x^2}{4(1+W_{v\parallel}^2)} + \frac{\theta_y^2}{4(1+W_{v\perp}^2)} \right), \quad (2.18)$$

where

$$W_{v\sigma} \equiv \frac{1}{2|\chi_g|P_\sigma} \left[\theta_x^2 + \theta_y^2 + \theta_{kin}^2 - \frac{|\chi_g|^2 P_\sigma^2}{\theta_x^2 + \theta_y^2 + \theta_{kin}^2} \right], \quad (\sigma = \parallel, \perp). \quad (2.19)$$

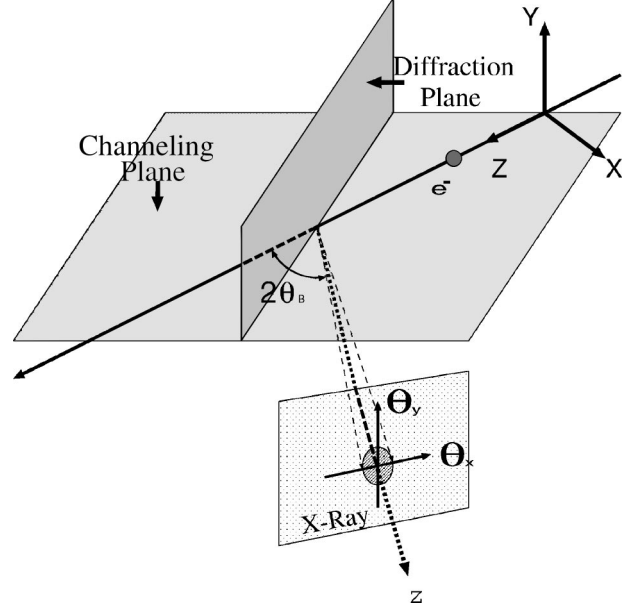


FIG. 1. Geometry of our system. The relativistic electron travels along the Z axis. The channel planes are parallel to the XZ plane. The θ_x, θ_y coordinates are also introduced to represent the angular distribution of the emitted photons. The Z axis indicates the direction satisfying the Bragg condition with respect to the beam direction. The diffraction plane is perpendicular to the channeling plane.

θ_x and θ_y are the angles of emission measured from the direction satisfying the Bragg condition (see Fig. 1), and $\theta_{kin}^2 = \gamma^{-2} + |\chi_0|^2$.¹³ In the above calculation, we have assumed that $\theta_{x,y} \ll 1$ is satisfied.

Next, we consider the interband transition corresponding to DCR. Using the dipole approximation $e^{-i(\mathbf{k}-\mathbf{g})_y y} \approx 1 - i(\mathbf{k}-\mathbf{g})_y y$ to Eq. (2.15), we obtain

$$M_{-\mathbf{g}}^{(if)} = \left(\frac{e}{c}\right) \langle \varphi_f | y | \varphi_i \rangle [i(\mathbf{k}-\mathbf{g})_y (\mathbf{A}_{-\mathbf{g}}^* \cdot \mathbf{v}_{\parallel}) + i(\mathbf{A}_{-\mathbf{g}}^*)_y \Omega_{if}] \times \delta(\mathbf{p}_{\parallel} - \mathbf{p}'_{\parallel} | \hbar \mathbf{k}_{-\mathbf{g}\parallel}). \quad (2.20)$$

Using Eq. (2.20), the radiation probability of DCR per unit length is obtained as

$$\left(\frac{dN}{d\theta_x d\theta_y dz} \right)_{DCR} = \frac{\alpha \omega_B^3 y_{if}^2}{4\pi c^3 \sin^2 \theta_B} \times \left(\frac{\theta_x^2 \theta_y^2}{4(1+W_{\parallel}^2)} + \frac{\left(\theta_y^2 - \frac{\Omega_{if}}{\omega_B} \right)^2}{4(1+W_{\perp}^2)} \right), \quad (2.21)$$

where α is the fine-structure constant $y_{if} = \langle \varphi_f | y | \varphi_i \rangle$,

$$W_\sigma = \frac{1}{2|\chi_g|P_\sigma} \left[R - \frac{|\chi_g|^2 P_\sigma^2}{R} \right], \quad (2.22)$$

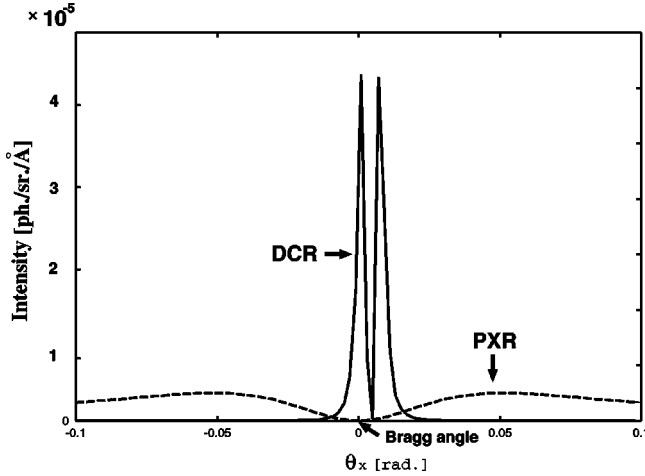


FIG. 2. Angular distribution of the intensity of DCR and PXR emitted by a 10-MeV electron channeled along the Si(110) plane. The diffraction plane is Si(1 $\bar{1}$ 1). The resonant condition is satisfied by the 1 \rightarrow 0 transition.

$$R = \left[\theta_x - \left(\frac{\Omega_{if}}{\omega_B} \right) \cot \theta_B \right]^2 + \theta_y^2 + \theta_{kin}^2 - 2 \left(\frac{\Omega_{if}}{\omega_B} \right). \quad (2.23)$$

W_σ corresponds to “the resonance error” in the theory of dynamical diffraction^{14,15} (also, see the appendix). In the next section, we discuss various properties of DCR in more detail by performing numerical calculations.

III. NUMERICAL RESULTS AND DISCUSSION

First of all, we note that an experimental condition for observing DCR is not as simple as that for PXR because the resonant condition depends on both the observation angle and the energy of the channeled electron.

As a typical example, we calculate the intensity of DCR for 8–20-MeV electrons channeled along the Si(110) plane. The incident angle to the channel plane is tilted 0.02° for obtaining enough population into the excited state $i=1$. The energy of the channeled electron is chosen so that the strongest CR peak appears in the x-ray energy region. From Eqs. (1.1) and (2.3), for the 1 \rightarrow 0 transition of a 10-MeV channeled electron, we obtain $\hbar\omega_B = 7.1$ keV for the (111) plane diffraction satisfying the resonant condition at the observation angle $\Theta = 2\theta_B = 32.2^\circ$. The channeling states have been obtained by the many-beam calculations. For $V(y)$, we have used the thermally averaged Doyle-Turner potential^{8,16} at $T = 300$ K.

In Fig. 2, we show a typical angular distribution of DCR. For comparison, the angular distribution of PXR is shown. The peak intensity of DCR is ten times stronger than that of PXR. In other numerical calculations, we have obtained up to a 10² enhancement at higher incident energies. The angular width of DCR is much narrower than that of PXR. This is because the width of PXR is of the order of θ_{kin} whereas for DCR it is of the order of $\sqrt{|\chi_g|}$, and $\theta_{kin} \gg \sqrt{|\chi_g|}$ is satisfied for MeV electrons.

Figure 3 shows the incident energy dependence of DCR. Below a certain energy, DCR is suddenly suppressed. This

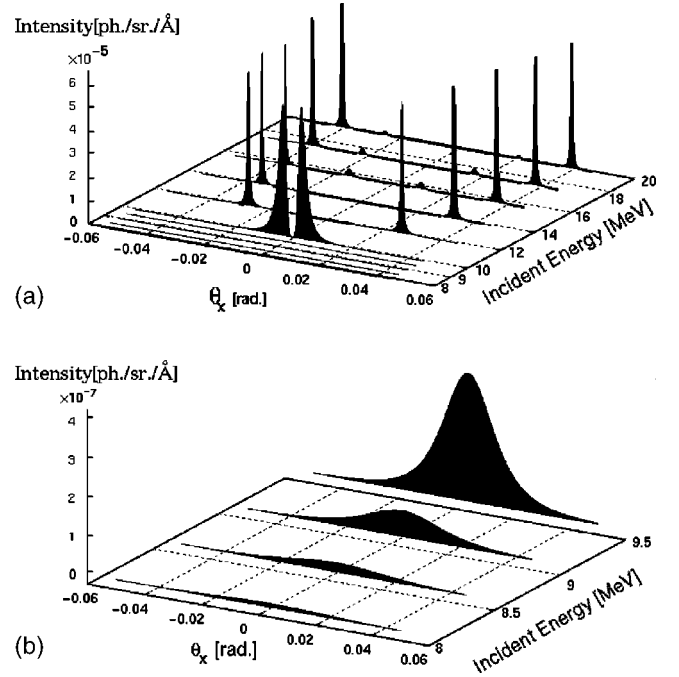


FIG. 3. (a) Angular distribution of DCR as a function of the incident energy. Other parameters are same as in Fig. 2. (b) The same as (a) but for lower energy. As the energy decreases below the threshold energy [Eq. (3.4)], DCR is suppressed very rapidly.

behavior is understood in terms of the energy dependence of the resonance error W_σ . Regarding W_σ as a function of θ_x , the solution of the equation $W_\sigma = 0$ is given by

$$\theta_x = \cot \theta_B \left(\frac{\Omega_{if}}{\omega_B} \right) \pm \sqrt{D}, \quad (3.1)$$

where

$$D = 2 \left(\frac{\Omega_{if}}{\omega_B} \right) - \frac{1}{\gamma^2} - |\chi_0| - \theta_y^2 \pm |\chi_g| P_\sigma. \quad (3.2)$$

When the condition $D < 0$ is satisfied, we have $W_\sigma > 0$ for all θ_x . Under this condition DCR is suppressed because, as one can see from Eq. (2.21), DCR becomes significant only at a certain narrow region of θ_x where $W_\sigma \approx 0$ is satisfied. On the other hand, when $D \geq 0$ is satisfied, two sharp DCR peaks arise at θ_x satisfying Eq. (3.1) for the 1 \rightarrow 0 transition. Each peak actually has a fine structure of the double peak similar to Fig. 2 because it has two maxima at the angles satisfying Eq. (3.1) while minima at

$$\theta_x = \cot \theta_B \left(\frac{\Omega_{if}}{\omega_B} \right) \pm \sqrt{2 \left(\frac{\Omega_{if}}{\omega_B} \right) - \frac{1}{\gamma^2} - |\chi_0| - \theta_y^2}, \quad (3.3)$$

which corresponds to the angles for $W_\sigma \rightarrow \infty$. The small peaks appearing at $E > 16$ MeV are associated with the 2 \rightarrow 1 transitions. Other transitions, e.g., 3 \rightarrow 2, are too small to be seen.

The above discussion suggests that we may introduce the threshold energy for observing DCR by

$$\gamma_{th} = \left[2 \left(\frac{\Omega_{if}}{\omega_B} \right) - |\chi_0| + |\chi_g| \right]^{-1/2}. \quad (3.4)$$

Neglecting the weaker dependence of Ω_{if} on γ , one may predict that a necessary condition for observing DCR is $\gamma > \gamma_{th}$. It would be worthwhile to mention that if both $|\chi_0|$ and $|\chi_g|$ are neglected, Eq. (3.4) recovers the ‘‘resonant condition’’ Eq. (1.1).

Finally, we consider PXRC. As mentioned in the previous section, the matrix element of PXRC, Eq. (2.16), differs from that of PXR in that it includes the form factor $F_{ii}[(\mathbf{k} - \mathbf{g})_y]$. The correction is very small for x rays. To see this, for simplicity, we assume that the diffraction plane is parallel to the θ_y axis ($\mathbf{g}_y = 0$). Since the angular distribution of PXRC has a width of the order of $1/\gamma$, it is similar to that of PXR. Thus we have $k_y \approx k \theta_y \lesssim k/\gamma$. In this case we may approximate that $\exp(-ik_y y) \sim 1 - ik_y y - (k_y y)^2$ and the form factor may be expanded as

$$F_{ii}(k_y) \sim F_{ii}(0) - \frac{k_y^2}{2} \langle \varphi_i | y^2 | \varphi_i \rangle \quad (3.5)$$

for the emission of x rays satisfying $k \sim d^{-1}$, where d is the lattice constant. From Eq. (3.5), we may conclude that the difference between PXR and PXRC is small because the contribution from the second term is less than of the order of $\gamma^{-2} \ll 1$. Indeed, our numerical calculation for 10-MeV electrons indicates that the second term in Eq. (3.5) is about 10^2 times smaller than the first term.

So far, we have neglected the inelastic collisions. In fact, a channeled electron is scattered by thermally displaced target atoms, target electrons, impurities, dislocations, etc. Due to the inelastic scattering the transverse state φ_i becomes unstable, having a finite lifetime τ_i . As is well known, this causes the linewidth in channeling radiation. DCR will be also affected by the inelastic scattering. One possible way to take into account the effect of channeling lifetime is to use simple exponentially decaying states¹⁶

$$\phi_i(y, t) = \varphi_i(y) e^{-t/2\tau_i}. \quad (3.6)$$

It should be noted, however, that this model will overestimate the effect especially for a thick target because rechanneling is not negligible at all. For detailed quantitative calculations, therefore, we should consider the population dynamics by using a master equation,¹⁶ which is outside the scope of our present paper.

IV. CONCLUSIONS

In this paper we have considered the effect of diffraction on channeling radiation from relativistic electrons. We have derived the frequency condition of the diffracted channeling radiation (DCR), which includes that of PXR and CR as special conditions. We have shown that PXR emitted by channeled electrons occurs as the intraband transition in the quantum transverse states whereas DCR occurs as the interband transition.

The numerical calculations for 10-MeV channeled electrons along Si(110) planes have shown that DCR intensity is about ten times stronger and the angular distribution is much

narrower than that of PXR. It should be noted that as the incident energy increases, the peak intensity ratio of DCR to PXR becomes larger, while the width of the DCR angular distribution becomes narrower.

It has also been shown that the incident energy dependence of DCR has a certain threshold. These properties of DCR will be helpful in discriminating between DCR and PXR experimentally. To observe DCR, the energy of channeled electrons should be in the quantum channeling region, i.e., typically $\lesssim 20$ MeV for planar channeling and $\lesssim 10$ MeV for axial channeling so that the principal CR is emitted at x-ray energies. In this paper we have considered DCR from planar-channeled electrons only, but it is straightforward to extend our theory to the case of axially channeled electrons as well as planar-channeled positrons.

ACKNOWLEDGMENT

One of the authors (H.N.) is grateful to Professor Yuri Pivovarov for stimulating discussions.

APPENDIX: DYNAMICAL DIFFRACTION OF X RAYS

The Maxwell equations describing the electromagnetic wave $\mathbf{A}(\mathbf{r})$ inside a crystal are given as

$$\text{div}[\varepsilon(\mathbf{r})\mathbf{A}(\mathbf{r})] = 0, \quad (A1)$$

$$\text{rot rot } \mathbf{A}(\mathbf{r}) - \left(\frac{\omega}{c} \right)^2 \varepsilon(\mathbf{r})\mathbf{A}(\mathbf{r}) = 0. \quad (A2)$$

Since the crystal has a periodic structure, the local dielectric function $\varepsilon(\mathbf{r})$ is also periodic. Therefore, we may expand it into the Fourier series as

$$\varepsilon(\mathbf{r}) = \varepsilon_0 + \varepsilon'(\mathbf{r}), \quad (A3)$$

$$\varepsilon'(\mathbf{r}) = \sum_{\mathbf{g}(\neq 0)} \chi_{\mathbf{g}} e^{i\mathbf{g} \cdot \mathbf{r}}, \quad (A4)$$

$$\chi_{\mathbf{g}} = - \frac{4\pi e^2}{m\omega^2} \rho_{\mathbf{g}}, \quad (A5)$$

where $\varepsilon_0 = 1 + \chi_0$ is the mean dielectric constant, $\chi_{\mathbf{g}}$ the Fourier component of the local electric susceptibility, and $\rho_{\mathbf{g}}$ the Fourier component of the electron density. According to the Bloch theorem, the wave function $\mathbf{A}(\mathbf{r})$ as a solution of Eqs. (A1) and (A2) becomes the Bloch wave

$$\mathbf{A}(\mathbf{r}) = \sum_{\mathbf{g}} \mathbf{A}_{\mathbf{g}} e^{i\mathbf{k}_{\mathbf{g}} \cdot \mathbf{r}} + \text{c.c.} \quad (A6)$$

Substituting Eqs. (A3)–(A6) for Eqs. (A1) and (A2), we obtain the fundamental equation of diffraction

$$\left[\frac{\mathbf{k}_{\mathbf{g}}^2}{K_0^2} - 1 - \chi_0 \right] \mathbf{A}_{\mathbf{g}} = \sum_{\mathbf{h}(\neq \mathbf{g})} \chi_{\mathbf{g}-\mathbf{h}} \mathbf{A}_{\mathbf{h}}, \quad (A7)$$

where $K_0 = \omega/c$.

When the Bragg condition associated with a reciprocal-lattice vector \mathbf{g} is satisfied, we may expect that the condition

$|\mathbf{A}_h| \ll |\mathbf{A}_0|, |\mathbf{A}_g|$ holds for $\mathbf{h} \neq 0, \mathbf{g}$. In this case we may use the two-wave approximation

$$\mathbf{A}(\mathbf{r}) \approx \mathbf{A}_0 e^{i\mathbf{k} \cdot \mathbf{r}} + \mathbf{A}_g e^{i\mathbf{k}_g \cdot \mathbf{r}}. \quad (\text{A8})$$

Then, from Eq. (A7), we obtain the two coupled equations

$$\left[\frac{\mathbf{k}_0^2}{K_0^2} - 1 - \chi_0 \right] \mathbf{A}_0 - \chi_{-g} \mathbf{A}_g = 0, \quad (\text{A9})$$

$$\left[\frac{\mathbf{k}_g^2}{K_0^2} - 1 - \chi_0 \right] \mathbf{A}_g - \chi_g \mathbf{A}_0 = 0. \quad (\text{A10})$$

By introducing the polarization vector $\mathbf{e}_{h\sigma}$, \mathbf{A}_h ($\mathbf{h}=0, \mathbf{g}$) is rewritten as

$$\mathbf{A}_h = \sum_{\sigma=\parallel, \perp} \mathbf{e}_{h\sigma} A_{h\sigma}, \quad (\text{A11})$$

where $\mathbf{e}_{h\sigma}$ is the polarization vector, and \parallel and \perp indicate the polarization direction parallel and perpendicular to the diffraction plane (i.e., the plane including both \mathbf{k}_0 and \mathbf{k}_g), respectively. For further simplicity, let us define ξ_h and P_σ as follows:

$$2\xi_h = \frac{\mathbf{k}_h^2}{K_0^2} - 1 - \chi_0, \quad (\text{A12})$$

$$P_\sigma = \begin{cases} \mathbf{e}_{0\perp} \cdot \mathbf{e}_{h\perp} = 1 & (\text{for } \sigma = \perp) \\ \mathbf{e}_{0\parallel} \cdot \mathbf{e}_{h\parallel} \approx \cos(2\theta_B) & (\text{for } \sigma = \parallel) \end{cases}. \quad (\text{A13})$$

Using Eqs. (A11)–(A13), Eqs.(A9) and (A10) may be rewritten in the form of the matrix equation

$$\begin{pmatrix} 2\xi_0 & -\chi_{-g} P_\sigma \\ -\chi_g P_\sigma & 2\xi_g \end{pmatrix} \begin{pmatrix} A_{0\sigma} \\ A_{g\sigma} \end{pmatrix} = 0. \quad (\text{A14})$$

Equation (A14) has nontrivial solutions only if the determinant of the matrix satisfies

$$4\xi_0 \xi_g - |\chi_g|^2 P_\sigma^2 = 0. \quad (\text{A15})$$

Under this condition, from Eq. (A14) we obtain the following relation between $A_{g\sigma}$ and $A_{0\sigma}$:

$$A_{g\sigma} = \frac{2\xi_0}{\chi_{-g} P_\sigma} A_{0\sigma} = \frac{\chi_g P_\sigma}{2\xi_g} A_{0\sigma}. \quad (\text{A16})$$

For describing the dynamical effect, it is convenient to introduce the ‘‘resonance error’’ W_σ defined by

$$W_\sigma = \frac{\mathbf{k}_g^2 - \mathbf{k}_0^2}{2K_0^2 |\chi_g| P_\sigma}. \quad (\text{A17})$$

Using W_σ , ξ_0 and ξ_g as the solutions of Eq. (A15) are given by

$$\xi_0^{(\pm)} = \frac{1}{2} |\chi_g| P_\sigma (-W_\sigma \pm \sqrt{1 + W_\sigma^2}), \quad (\text{A18})$$

$$\xi_g^{(\pm)} = \frac{1}{2} |\chi_g| P_\sigma (W_\sigma \pm \sqrt{1 + W_\sigma^2}). \quad (\text{A19})$$

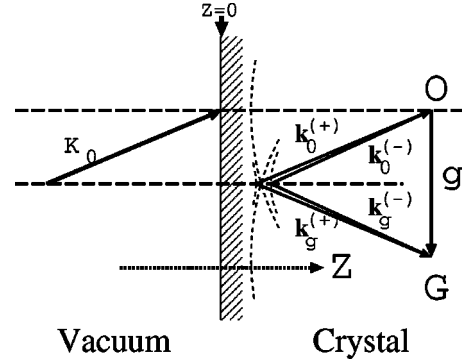


FIG. 4. The boundary condition for the x-ray incident on a crystal near the Bragg condition (the Laue case). Inside the crystal, x rays are excited onto the two branches (+) and (−) due to the dynamical effect. $\mathbf{k}_0^{(\pm)}$ and $\mathbf{k}_g^{(\pm)}$ represent the primary waves and the diffracted waves, respectively.

Next, we consider the boundary condition that determines the amplitude of the internal field excited by the external field. The external field is written as

$$\mathbf{A}_\sigma^{(0)}(\mathbf{r}) = A_{0\sigma}^{(0)} \mathbf{e}_{0\sigma} e^{i\mathbf{k}_0^{(0)} \cdot \mathbf{r}} + \text{c.c.}, \quad (\text{A20})$$

while the internal field as

$$\begin{aligned} \mathbf{A}_\sigma(\mathbf{r}) = & A_{0\sigma}^{(+)} \mathbf{e}_{0\sigma} e^{i\mathbf{k}_0^{(+)} \cdot \mathbf{r}} + A_{0\sigma}^{(-)} \mathbf{e}_{0\sigma} e^{i\mathbf{k}_0^{(-)} \cdot \mathbf{r}} + A_{g\sigma}^{(+)} \mathbf{e}_{g\sigma} e^{i\mathbf{k}_g^{(+)} \cdot \mathbf{r}} \\ & + A_{g\sigma}^{(-)} \mathbf{e}_{g\sigma} e^{i\mathbf{k}_g^{(-)} \cdot \mathbf{r}} + \text{c.c.}, \end{aligned} \quad (\text{A21})$$

where we have approximated the direction of the polarization vectors as $\mathbf{e}_{g\parallel}^{(+)} \approx \mathbf{e}_{g\parallel}^{(-)}$ because the difference is of the order of $|\chi_g|$. In the above, (+) and (−) imply the wave on the upper branch and on the lower branch, respectively. The relation between the external field and the internal field is schematically shown in Fig. 4. At the surface ($z=0$). Since the \mathbf{g} wave appears only inside the crystal, the boundary condition may be given as

$$A_{0\sigma}^{(0)} = A_{0\sigma}^{(+)} + A_{0\sigma}^{(-)}, \quad (\text{A22})$$

$$0 = A_{g\sigma}^{(+)} + A_{g\sigma}^{(-)}. \quad (\text{A23})$$

Then, from Eqs. (A16), (A22), and (A23), each component of the internal field is expressed by the external field. Using W_σ , we obtain

$$A_{0\sigma}^{(+)} = \frac{1}{2} \left(1 + \frac{W_\sigma}{\sqrt{1 + W_\sigma^2}} \right) A_{0\sigma}^{(0)}, \quad (\text{A24})$$

$$A_{0\sigma}^{(-)} = \frac{1}{2} \left(1 - \frac{W_\sigma}{\sqrt{1 + W_\sigma^2}} \right) A_{0\sigma}^{(0)}, \quad (\text{A25})$$

$$A_{g\sigma}^{(+)} = -\frac{1}{2} \frac{1}{\sqrt{1 + W_\sigma^2}} A_{0\sigma}^{(0)}, \quad (\text{A26})$$

$$A_{g\sigma}^{(-)} = \frac{1}{2} \frac{1}{\sqrt{1+W_{\sigma}^2}} A_{0\sigma}^{(0)}. \quad (\text{A27})$$

These expressions have been used for the calculations of \mathbf{A}_g appearing in Sec. II C. For obtaining the field corresponding to the emitted photon, the reciprocity theorem has been applied.¹⁷

*Corresponding author.

- ¹U. Nething, M. Galemann, H. Genz, M. Höfer, P. Hoffmann-Stascheck, J. Hormes, A. Richter, and J.P.F. Sellschop, *Phys. Rev. Lett.* **72**, 2411 (1994).
- ²H. Nitta, in *New Perspectives on Problems in Classical and Quantum Physics, Part I: Radiation and Solid State Physics, Nuclear and High Energy Physics, Mathematical Physics*, edited by P. P. Delsanto and A. W. Sáenz (Gordon and Breach, New York, 1998), p. 175.
- ³V.G. Baryshevsky and I.Ya. Dubovskaya, *J. Phys. C* **16**, 3663 (1983).
- ⁴T. Ikeda, Y. Matsuda, H. Nitta, and Y. H. Ohtsuki, *Nucl. Instrum. Methods Phys. Res. B* **115**, 380 (1996). It should be noted that, in Refs. 4 and 5, we had used the term ‘‘PXRC’’ for DCR. We made the change for the purpose of distinguishing the interband process from the intraband one.
- ⁵Y. Matsuda, T. Ikeda, H. Nitta, and Y. H. Ohtsuki, *Nucl. Instrum. Methods Phys. Res. B* **115**, 396 (1996).
- ⁶H. Nitta, *Phys. Lett. A* **158**, 270 (1991).
- ⁷J. U. Andersen, *Nucl. Instrum. Methods* **170**, 1 (1980).
- ⁸A. W. Sáenz and H. Überall, *Coherent Radiation Sources*

(Springer-Verlag, New York, 1985).

- ⁹For suggesting the term ‘‘diffracted coherent bremsstrahlung,’’ we would like to thank an anonymous referee.
- ¹⁰Using Eq. (2.12) we may rewrite the form factor as $F_{ii}(q) = \sum_{G,G'} C_{G'}(p'_y) C_G(p_y) \delta[p_y - p'_y | \hbar(q + G - G')]$. In the plane-wave limit, we have $C_G(p_y) = \delta(G|0)$.
- ¹¹H. Nitta, *Nucl. Instrum. Methods Phys. Res. B* **115**, 401 (1996).
- ¹²H. Nitta, *J. Phys. Soc. Jpn.* **69**, 3462 (2000).
- ¹³Equation (2.18) may be rewritten in a somewhat simpler expression, see Ref. 12. Here we use this expression with the ‘‘resonance error’’ W for emphasizing the relation with the formulas conventionally used in the dynamical theory of diffraction.
- ¹⁴Y. H. Ohtsuki, *Charged Beam Interaction with Solids* (Taylor & Francis, London, 1983).
- ¹⁵Z. G. Pinsker, *Dynamical Scattering of X-Rays in Crystals* (Springer-Verlag, New York, 1977).
- ¹⁶J. U. Andersen, E. Bonderup, E. Laegsgaard, and A. H. Sorensen, *Phys. Scr.* **28**, 303 (1983).
- ¹⁷P. Rullhusen, X. Artru, and P. Dhez, *Novel Radiation Sources Using Relativistic Electrons* (World Scientific, Singapore, 1998).